A MODEL STUDY OF TRANSVERSE MODE COUPLING INSTABILITY AT NATIONAL SYNCHROTRON LIGHT SOURCE-II (NSLS-II)

Alexei Blednykh and Jiunn-Ming Wang, BNL, NSLS, Upton, New York, 11973-5000, USA

Abstract

The vertical impedances of the preliminary designs of National Synchrotron Light Source II (NSLS-II) Mini Gap Undulators (MGU) are calculated by means of GdfidL code. The Transverse Mode Coupling Instability (TMCI) thresholds corresponding to these impedances are estimated using an analytically solvable model.

INTRODUCTION

Up to twenty mini-gap undulators (MGUs) with 5 mm magnet gaps are envisioned to be the major source of light at NSLS-II. In order for NSLS-II to be successful, we have to make sure that TMCI induced by MGUs is under control. We compute the transverse impedance for some model MGUs and estimate the threshold for the corresponding TMCI.

For numerical calculations of the vertical impedance, the 3D computer code GdfidL [1] is used. GdfidL runs on Linux cluster with 6 AMD64 CPUs and 10 gigabyte RAM.

For threshold estimation, the machine and beam parameters of [2] will be adopted throughout this paper. We approximate the computed impedance by a broadband impedance (BBZ) of quality factor Q_r =1. For a transverse resonance, Imaginary[$Z(\omega\rightarrow 0)$] = $\mathcal{R}/Q_r$, where $\mathcal{R}$ is the shunt impedance; therefore we shall use these two quantities interchangeably.

VERTICAL IMPEDANCE OF MGUS MODEL

We first treat a preliminary design of superconducting (SC) MGU. The vacuum chamber in the magnet section of the SCMGU has a small elliptical beam pipe with full major axis a_s=15mm and full minor axis b_s=5mm; the length L_m of the magnet section is 5m. Each side of the small beam pipe is connected to the regular beam pipe (a_b=50 mm and b_b=25 mm) by a half-meter long taper.

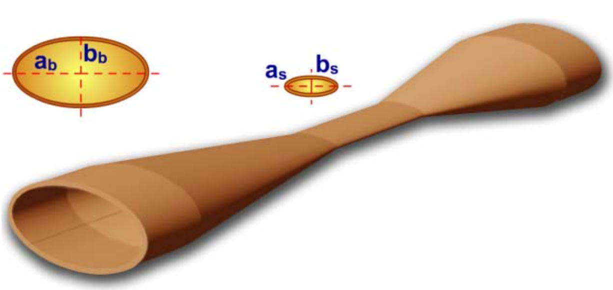

Figure 1: Elliptic vacuum chamber of the SCMGU.

For L_m= 5m, the available computer resource does not allow us to take a small enough step size. Fortunately, computation for this MGU in the accessible region indicates that Im[$Z(\omega\rightarrow 0)$] is independent of L_m. We assume that this is the case all the way up to L_m= 5m. GdfidL results are presented in Figure 2. The parameters used: Taper length = 500mm, L_m = 100mm and regular beam pipe length = 50mm, totally 1.2 m. With step size 100µm, the frequency range of computations is limited to f <110GHz. From Fig. 2, Im[$Z(\omega\rightarrow 0)$] = 6.5 kΩ/m.

Note the prominent resonant structure of Z in Fig. 2. Theoretical consideration leads us to believe that most of them are TE-mode resonances trapped by the tapers in the magnet section. Detailed discussion on these trapped modes will be presented elsewhere [3].

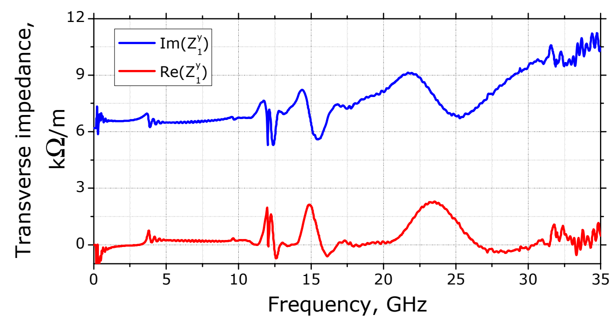

Figure 2: Real and imaginary part of the transverse impedance for the vacuum chamber of SCMGU.

We next consider the vertical impedance of a room-temperature (RT) MGU. The design of this MGU is similar to the 3.3 mm gap MGU currently being used at X-Ray ring of NSLS [4,5]. A simplified cut out picture of such RTMGU is shown in Fig. 3. It consists of two magnet arrays placed in a rectangular vacuum chamber. Two sides of the permanent magnet section are connected to the tapers by means of the tensile plates. The tapers are fixed relative to the vacuum chamber, however the tensile plates are flexible, allowing the gap between the two magnets in the vacuum chamber to vary. We note that the cross section of the permanent magnet section looks like an H-wave guide.

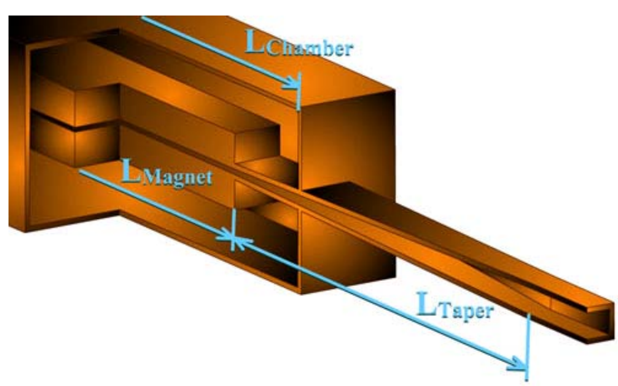

Figure 3: Room Temperature MGU.

The dimensions of various parts of the RTMGU for NSLS-II are as follows: The width and the height of the vacuum chamber are 0.2m and 0.16m, respectively; the magnet width = 0.1m; magnet length = 5m; the taper length = 0.5m.

In Figure 4 are shown GdfidL-computation results of the reactive part of Z up to f = 4 GHz for two magnet lengths 390mm and 2000mm. We did not compute for the designed value of the magnet length 5m due to the limitation of the available computer resource. Corresponding to the step size of 500µm, the maximum frequency we can deal with is 50GHz. We mention here that Im[Z] is inductive and increasing with increasing f at f = 50 GHz, which implies that the resonance frequency f_{BB} of the broadband impedance is greater than 50 GHz.

A series of resonances are clearly visible in Figure 4. Up to frequency 1GHz they correspond to the TE_{10p} modes in the H waveguide and to the TE_{11p} modes in the coaxial waveguide, where p is the number of field variations in the z-direction. As we expect, the number of such resonances in a frequency range is proportional to the magnet length.

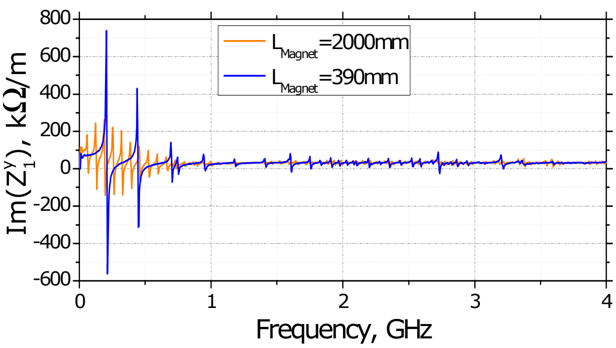

Figure 4: Imaginary parts of the transverse impedances for magnet lengths 390 mm and 2000 mm (RTMGU).

The imaginary parts of the transverse impedances at low frequencies are ~ 70 kΩ/m for the magnet length 390mm and ~ 100 kΩ/m for the magnet length 2000 mm (with a step size of 500µm). Transverse impedance in such a structure depend on the magnet length, and the impedance increases with increasing L_m. A linear extrapolation gives ImZ(ω→0) ~ 155 kΩ/m for L_m = 5m.

The total R/Q_r for twenty 5m RTMGU above is ~3MΩ/m; this is too big. Two options for reducing this number are considered. In the first one, flexible metallic Ω-form insertion is added between the top and the bottom of the magnets. The tensile plates have a metallic shield. This reduced the vertical impedance to 43kΩ/m (with a step size 500µm). We conjecture, based on our experience, that had we enough computer resources to calculate with a step size of 100 µm, we would have obtained ~ 27kΩ/m. For this shielded geometry the imaginary part of the transverse impedance does not depend on the magnet length.

For the second option, we added damping material silicon carbide (SiC) in the RTMGU structure. We found that the amount of reduction in ImZy(ω→0) is negligible if we insert SiC in the magnet section. An effort to add the damping material to the tapers is in progress.

THRESHOLD ANALYSIS

We estimate in the remainder of the paper the effects of the MGUs considered above on TMCI. We employ a solvable model where only the rigid dipole mode corresponding to µ = 0 and the dipole mode µ = -1 contribute. The method is based on Ruth's asymptotic expansion of the dispersion relation for vertical coherent motion [6,7]. As mentioned earlier, we take the vertical impedance Z(ω) to be a broadband impedance (BBZ) with the quality factor Q_r = 1. Instead of Z, it is convenient to use a dimensionless quantity $\bar{Z}(\omega) = Z(\omega)/R$, where R is the shunt impedance. We shall also use the effective impedance defined by

$$\zeta_k = \sum \exp(-\psi_m^2)(\psi_m/\sqrt{2})^k \bar{Z}[(m+\delta\nu_y)\omega_0],$$

where $\psi_m = (n+\delta\nu_y)\omega_0\sigma_\tau$ (for simplicity we assume the chromaticity ξ = 0 in this paper), $\delta\nu_y$ is the fractional part of the vertical tune ν_y, and the summation is from $m = -\infty$ to ∞. Since Z is a broadband impedance, ζ_k can, from the symmetry property of Z, be regarded to a very good approximation, as purely reactive when k is an even integer, and resistive when k is odd. Let us introduce the notation $\bar{L}_k$ = –Im[ζ_k] when k is even, and $\bar{R}_k$ = Re[ζ_k] when k is odd.

The coherent modes are solutions of the following eigenvalue equation:

$$\begin{pmatrix} -i\eta\bar{L}_0/q, & -i\eta\bar{R}_1/(1+q) \\ -i\eta\bar{R}_1/q, & -i\eta\bar{L}_2/(q+1) \end{pmatrix} \begin{pmatrix} u_0 \\ u_{-1} \end{pmatrix} = \begin{pmatrix} u_0 \\ u_{-1} \end{pmatrix}, \quad (1)$$

where q is the coherent frequency shift normalized by ω_s, the dimensionless quantity $\eta = \lambda I_B$, I_B is the bunch current and $\lambda = cR/4\pi E_0\nu_y\omega_s$. Note that the diagonal elements of the matrix are reactive and the off-diagonal elements are resistive. Also that if we ignore the off diagonal elements of the above matrix, the eigenvalues are q = - $i\eta\bar{L}_0$ and -1-$i\eta\bar{L}_2$.

An eigenvalue q is a solution of the quadratic secular equation

$$q^2 + q\,[1+\eta\,(\bar{L}_0+\bar{L}_2)] + [\eta\,\bar{L}_0 + \eta^2\,(\bar{L}_0\,\bar{L}_2+\bar{R}_1^2)] = 0, \quad (2)$$

and the positive imaginary part of q corresponds to instability. The threshold condition can readily be obtained from the above equation as

$$(R/Q_r)_{th} = 4\pi E_0\nu_y\omega_s/\,[cI_B\,(\bar{L}_0-\bar{L}_2+2\,\bar{R}_1)]. \quad (3)$$

In the limit of $f_{BB} \to \infty$, where f_{BB} is the resonance frequency of BBZ, the above expression becomes

$$(R/Q_r)_{th} = (16\sqrt{\pi}/3)(E_0\nu_y\sigma_\tau\omega_s\omega_0/cI_B). \quad (4)$$

0-7803-8859-3/05/$20.00

This expression set a very convenient scale for the TMCI threshold.

TMCI THRESHOLD AT NSLS-II

We apply the threshold analysis above to NSLS-II. Using the nominal value I_B = 0.7 mA and other NSLS-II parameters [2], we obtain Figure 5, where the threshold value of R/Q_r in units of MΩ/m is plotted as a function of f_{BB} in the range of 50 GHz < f_{BB} < 200 GHz. Recall that we do not know the exact value of f_{BB}, except that it is greater than 50 GHz; we conclude from this and Figure 5 that

$$0.9\ \mathrm{M\Omega/m} < (R/Q_r)_{th} < 1.14\ \mathrm{M\Omega/m}. \qquad (5).$$

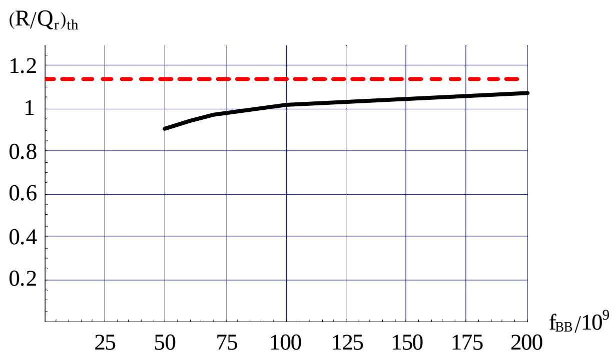

Figure 5: Dependence of R/Q_r threshold f_{BB}.

Note that, in Figure 5, $(R/Q_r)_{th}$ = 0.9MΩ/m at f_{BB}=50GHz. Figure 6 compares the TMCI plot for the above point with that for R/Q_r = 0.9MΩ/m and f_{BB}= ∞. The difference of the threshold currents is about 20%.

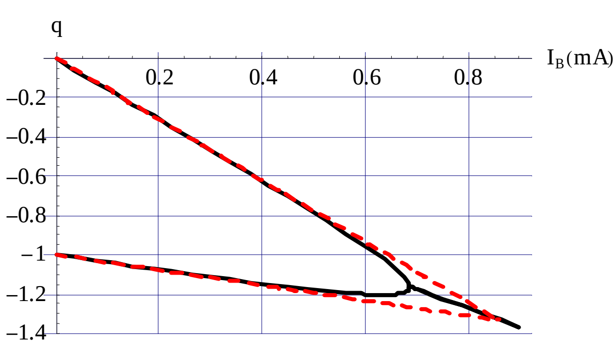

Figure 6: TMCI threshold for a bunch current. Two-mode model.

As mentioned earlier, we consider installing up to 20 MGUs in NSLS-II. If we compare the results of Section 2 with Eq.(5), we see that TMCI is above threshold for 20 unshielded RTMGU, but it is below threshold for the same number of shielded RTMGU or SCMGU.

One important question remains: The two-mode approximation should be pretty good for small f_{BB}, but how good is it in the frequency region under consideration. In Figure 7, we compare the TMCI plot of two-mode model and that of nine-mode model. The parameters used are f_{BB} = 150 GHz, and R/Q_r = 0.9MΩ/m. The black lines correspond to two-mode model, and the blue lines to nine-mode model. We see the difference in the threshold currents is about 25%. We take this to be the range of error for the two-mode model.

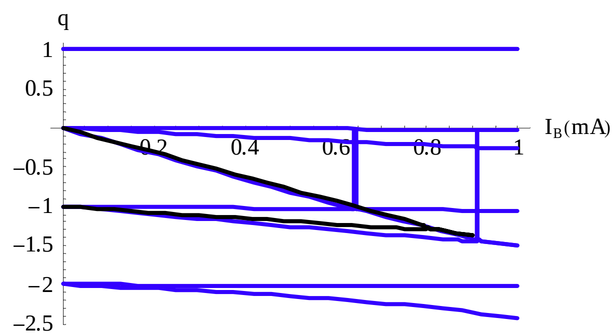

Figure 7: TMCI plots for nine-mode model and two-mode model.

CONCLUSION

By choosing long tapers and, for RTMGU, shielding the beam chamber from the resonances associated with the H-waveguide, we succeeded in designing MGU beam chambers with acceptable vertical beam impedance.

ACKNOWLEDGEMENT

We thank W. Bruns for guiding us in the usage of GdfidL. The advice from G. Rakowsky and T. Tanabe about MGU design was indispensable for the progress of this paper. We benefited from comments by I. Pinayev and J. Rose. One of us (jmw) thanks R. Nagaoka and Y.C. Chae for initiating him to the world of TMCI phenomenology.

NOTICE

REFERENCES

[1] W. Bruns. http://www.gdfidl.de
[2] B. Podobedov et al, PAC03, p.241.
[3] A. Blednykh, J. M. Wang, To be published.
[4] P.M. Stefan, S. Krinsky, G. Rakowsky, L. Solomon, NSLS Prototype Small-Gap Undulator", PAC 1991, San Francisco, California, 6-9 May 1991.
[5] G. Rakowsky, D. Lynch, E.B. Blum and S. Krinsky, NSLS in-vacuum undulators and mini-beta straights", PAC 2001, Chicago, 18-22 June 2001.
[6] R. Ruth, BNL/ISA 81-4, See also J. M. Wang and Ruth, PAC81, p2405.
[7] K. Satoh and Y. Chin, NIM **207** (1983) p309.